Nematic-Isotropic Transition with Quenched Disorder

L. Petridis and E. M. Terentjev
Cavendish Laboratory, University of Cambridge
J J Thomson Avenue, Cambridge CB3 0HE, UK
(Dated: February 6, 2008)

Nematic elastomers do not show the discontinuous, first-order, phase transition that the Landau-De Gennes mean field theory predicts for a quadrupolar ordering in 3D. We attribute this behavior to the presence of network crosslinks, which act as sources of quenched orientational disorder. We show that the addition of weak random anisotropy results in a singular renormalization of the Landau-De Gennes expression, adding an energy term proportional to the inverse quartic power of order parameter Q. This reduces the first-order discontinuity in Q. For sufficiently high disorder strength the jump disappears altogether and the phase transition becomes continuous, in some ways resembling the supercritical transitions in external field.

to be published on *Phys. Rev. E*

PACS numbers: 61.30.Dk, 75.10.Nr, 61.41.+e

I. INTRODUCTION

Although there is a large volume of literature devoted to the effects of quenched disorder, there has been relatively little study on how it influences the behavior of systems whose pure versions undergo a first-order phase transition. This question was first addressed by Imry and Wortis [1] who showed that inhomogeneities may cause local variations of the transition temperature inside the sample. Provided that the cost in interface energy is not great, bubbles of the "wrong" phase are formed, eventually leading to a substantial rounding of the transition. A theorem due to Aizenman and Wehr [2] shows that in less than two dimensions there can be no phase coexistence at the transition, and therefore no latent heat, in a system with quenched random impurities. Therefore these systems are expected to always exhibit a continuous transition.

The influence of quenched impurities coupling to the local energy density has been extensively studied by Cardy [3, 4]. A mapping to the random field Ising model, whose renormalization group flows are well known, addresses the question of what happens in higher than two dimensions where the Aizenman-Wehr theorem is not applicable. It was found that, depending on the specific values of parameters such as the laten heat and the surface tension, the phase transition can either be first or second order. More conclusive analytic results were obtained in an Ising model with discrete order parameter [3]. The pure system exhibits a fluctuation-driven first order transition, where the mean field theory predicts a continuous transition but fluctuation effects make it discontinuous. Quenched randomness eventually drives the transition to become continuous in two dimensions, in accordance with the Aizenman-Wehr theorem, but this may or may not happen in higher dimensions.

The majority of studies in this field are carried out for spin-glass or analogous systems, e.g. with a frustrated dipolar ordering [5, 6]. However, in such systems the experimental work is difficult and results are often indirect. In contrast, the quadrupolar orientational ordering of nematic liquid crystals offers the easy experimental access to thermodynamic and structural features of phase transitions. The classical work on frustrated nematic liquids by Bellini et al. [7, 8] has generated a large interest in studies of liquid crystals in random environments, such as porous silica gel. One must appreciate, however, that the characteristic length scale of such disorder is much greater than the coherence length of the nematic order parameter and thus the theoretical concept of a continuous coarse-grained random field [9] is difficult to sustain.

Quenched disorder is intrinsically present in nematic elastomers as a direct result of their synthesis [10, 11]. Sources of disorder are introduced by crosslinking a liquid-crystalline polymer melt. In the simplest situation, the crosslinking takes place in the isotropic phase, in which case the local anisotropy axis of each crosslinking moiety is randomly oriented. Once the polymer network is formed, the configuration of the crosslinks remains quenched, that is, it does not change with time and temperature. Unless special precautions are taken during network fabrication, the low temperature (ordered) phase of nematic elastomers is always an equilibrium polydomain director texture [12, 13]. This is in marked contrast with a kinetic "polydomain" texture often referred to as Schlieren texture [14], which is the consequence of nucleation and growth mismatch in a system undergoing the first-order transition [15]. The equilibrium polydomain structure of nematic elastomers is reversible with changing temperature and is characterized by the uniform non-zero order parameter, but the highly non-uniform orientation of the principal axis of nematic director $\boldsymbol{n}$. Correlations between directors decay rapidly and eventually vanish at distances much larger than ξ, the correlation length or domain size. This is in agreement with the general result that quenched impurities destroy long-range order, first shown by Larkin [16] and then generalized by Imry and Ma [9]. There is a full anal-

ogy with a corresponding dipolar system named "random anisotropy magnets" [17, 18, 19]. In fact, all other (e.g. smectic [20]) liquid crystal elastomers follow the same pattern of forming the equilibrium textures with a characteristic length scale often referred to as the domain size.

This length scale in typical nematic elastomers is of the order of microns [12, 13], therefore light passing through the sample is multiply scattered on birefringent domains with randomly oriented optical axis [21] (see [10] for a brief review of experimental facts in this area). As a result such a sample is completely transparent at high temperatures, but becomes opaque below its nematic-to-isotropic transition temperature T_{NI}. It should be noted that the polydomain texture is the thermodynamically stable low-temperature phase. Applying an adequately strong aligning stress [12] or increasing the temperature above T_{NI} [13] destroys the polydomain texture, by aligning the local axis of each domain, or removing the optical contrast between them. However, once the stress is removed (or the temperature lowered), the elastomer returns to its previous state and the average domain size is found to be reversible during this stress (or temperature) cycling.

Experimental investigations in nematic elastomers support the theoretical ideas of a continuous nematic-isotropic transition, rather than the discontinuous first-order transition expected by the Landau-De Gennes mean field theory based on the symmetry of quadrupolar ordering in three dimensions. The fact that polydomain nematic textures are optically opaque creates a practical problem when attempting to experimentally determine the local order parameter Q of the mesogenic units. It is impossible to use birefringence, dichroism or Xray measurements, the methods that have made this task simple in aligned liquid-crystal systems. Nuclear magnetic resonance (NMR) provides perhaps the only opportunity of order detection, by tracking the bias in orientational motion of selected chemical bonds and providing a unique Q-signature even in the orientationally averaged case. It was used to measure $Q(T)$ of both a nematic polymer melt and its corresponding crosslinks network [22, 23]. The addition of crosslinks was shown to make the nematic transition smooth, as well as to slightly reduce order. An indirect alternative to NMR comes from applying an external field to align the domains. Birefringence can then be measured, as long as the system has passed the critical point of the polydomain-monodomain transition [19]. The order parameter can thus be found for a series of decreasing applied fields. Although the zero-stress limit is not accessible, it can be extrapolated from the comparison of the other curves and, again, a continuous phase transition is seen [24].

The continuous transition is also found in carefully synthesized monodomain nematic elastomers, where a second stage of the crosslinking takes place when the sample is stressed [25]. Plots of the macroscopic order parameter $Q(T)$, obtained through birefringence [26], X-ray scattering [27] and NMR measurements [23], show the same behavior. There are two possible explanations for such a deviation from the basic symmetry-based expectation of a first-order transition. Inhomogeneities may cause local variations of the transition temperature inside the sample and lead to a substantial rounding of the transition, as discussed in [1]. The other explanation considers stresses imprinted in the system during the second crosslinking stage, which add a $-fQ$ term to the Landau-De Gennes expansion. Obviously, for adequately large f, the system would become supercritical and show a continuous transition. The analysis of the NMR spectra supports the supercritical scenario, although some degree of inhomogeneity was also found using the second moment of the spectra [23]. Another study of strain as a function of temperature over a range of applied tensile stress argues the opposite point [28]. The blurring of the isotropic-nematic transition is attributed to the presence of heterogeneities, although the authors do not consider boundary effects that are bound to be present as discussed in [1].

Uchida [29] has studied disordered polydomain nematic elastomers with emphasis on the role of nonlocal elastic interactions. He has shown that networks crosslinked in the isotropic phase lose their long-range orientational order due to the locally quenched random stresses, which were incorporated into the affine-deformation model of nematic rubber elasticity. Simulation work was carried out to investigate the role of random bonds and random fields that might be present in elastomers [30], in both cases finding that the first-order isotropic-nematic transition to broaden into a smooth crossover. For random-field disorder, the smooth crossover into an ordered state is also attributed to the long-range elastic interaction present in elastomers. A recent coarse-grained model for liquid-crystalline elastomers has also found that both homogeneous and inhomogeneous samples undergo a continuous isotropic-nematic transition [31].

In this paper we apply the traditional spin-glass techniques to investigate the characteristics of nematic phase transition in a system with quenched random anisotropy. The structure of the paper is as follows. In Section II we summarize a physical model of quenched disorder in nematic systems following [19], and introduce the replica Hamiltonian. Section III applies the auxiliary fields to incorporate several constraints into this problem and obtains the effective mean-field free energy of disorder in the system. In Section IV we investigate the stability of replica symmetry and discover the limits where our solutions are valid. Finally, in Section V we obtain the final free energy renormalization in terms of the order parameter Q and disorder strength, and investigate the characteristics of the nematic phase transition in various situations. We conclude by discussing our results and comparing them with experiments.

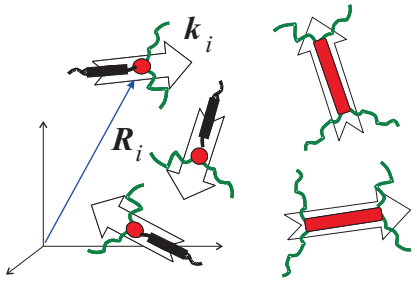

FIG. 1: Schematic representation of how crosslinks provide easy anisotropy axes $\{\mathbf{k}\}$. The nematic director is forced to be aligned, in the vicinity of the crosslink, with the axes, which are represent by the arrows. Both the orientation of $\{\mathbf{k}\}$ as well as the positions of the crosslinks $\{\mathbf{R}_i\}$ are random. Since the crosslinks are confined by the network topology, they add quenched disorder to the nematic system.

II. MODEL

A. Sources of Quenched Disorder

In the case of nematic elastomers crosslinked in the isotropic phase, the sources of quenched disorder are provided by the network crosslinks. Almost independently of their specific chemical structure, the crosslinks contain anisotropic groups that locally provide easy anisotropy axes $\boldsymbol{k}$: it is favorable for the local director to align along $\boldsymbol{k}$ in the vicinity of the crosslink because the anisotropic molecules in both the crosslinkers and in the nematic system interact, both sterically and via the long-range van de Waals attraction. The local anisotropy axes of the crosslinks, as well as their distribution inside the sample, are quenched variables since the crosslinks can neither rotate nor move once the chemical synthesis of the elastomer is complete. Although this has never been tested experimentally, there are two independent molecular models that estimate the energy of orientational confinement that a crosslink experiences from the surrounding network strands [32, 33]

We follow earlier work [10] in modelling the local coupling of the nematic order and the random field applied by the crosslinks. For a crosslink positioned at $\boldsymbol{R_i}$, with an anisotropy axis $\boldsymbol{k_i}$, an energy $-\gamma\, \boldsymbol{k_i} \cdot \underline{\underline{\boldsymbol{Q}}} \cdot \boldsymbol{k_i}$ is raised due to the interaction with the local nematic order parameter $Q_{ij} = Q\,(n_i n_j - \delta_{ij}/3)$, where γ is the coupling strength. Employing a coarse-grained expression for the continuum density of crosslinks $\rho\,(\boldsymbol{r}) = \sum_{\boldsymbol{R_i}} \delta(\mathbf{r} - \mathbf{R_i})$ and substituting the full tensor expression for $\underline{\underline{\boldsymbol{Q}}}$, we get the random field energy:

$$F_{\text{r.f.}} = -\int d^3\boldsymbol{r}\, \gamma\, Q\, \rho(\boldsymbol{r})\, (\boldsymbol{k}\cdot\boldsymbol{n})^2, \qquad (1)$$

where the irrelevant constant $\gamma \int \rho(\boldsymbol{r})$ has been dropped. Although the random field energy is proposed specifically for a nematic elastomer, it is a general expression which is valid for all random-anisotropy systems with underlying quadrupolar symmetry.

To obtain the full Hamiltonian describing the nematic ordering, the gradient elasticity penalizing the fluctuations of the director field must be also taken into account. In continuum elasticity the Hamiltonian takes the form:

$$H[\rho, \boldsymbol{k}] = \int d^3\boldsymbol{r} \left[\frac{K}{2}\,(\nabla \boldsymbol{n})^2 - \gamma\, Q\, \rho\, (\boldsymbol{k}\cdot\boldsymbol{n})^2\right], \qquad (2)$$

where K is the Frank elastic constant in the one-constant approximation. A simple dimensional argument gives $K \sim k_B T/a$, where a is the nematic coherence length, below which the meanings of the director n and order parameter Q are ill-defined [14]. Both microscopic and phenomenological theories of nematic-isotropic transition give the elastic constant K to scale as Q^2 for $Q \ll 1$. Combining these two estimates, we take that for small Q the elastic constant is approximately given by $K \simeq k_B T Q^2/a$. It is important to clarify that we are examining a homogeneous sample and as a result the magnitude of Q and the T_{NI} are uniform across the sample. There is a rich literature on the role inhomogeneities play in general first-order systems [1] and more specifically in nematic elastomers [28, 29, 30, 34]. The important difference in our assumptions is that, although the director correlations in the polydomain nematic are short-range (equilibrium spin-glass texture), the underlying nematic order parameter Q is homogeneous across the system. This assumption is based on the fact that the spin-glass like nematic textures are in fact homogeneous, in the sense that every element of the sample is equivalent to others: no 'domain walls' (unlike, for instance, during the stress-induced poly-monodomain transition [10] when the domain walls localize).

B. The Replica Method

There are three established methods of dealing with quenched random fields in the replica method framework: one based on the functional renormalization group analysis, another using the Gaussian variational method and the third using auxiliary fields. This paper employs the latter.

We are interested in results that do not depend on the specific distributions of $\rho(\boldsymbol{r})$ and $\boldsymbol{k}$ because we cannot control these distributions experimentally. In other words we are looking for the free energy averaged over the random distributions of the quenched variables $\rho(\boldsymbol{r})$ and $\boldsymbol{k}$. Crosslinking the sample above T_{NI} makes the easy anisotropy axes point at random directions, with an isotropic probability of orientation $P(\boldsymbol{k}) = \frac{1}{4\pi}$. Furthermore, the crosslinks are dispersed randomly in the sample with density ρ. The probability that a particular distribution $\rho(\boldsymbol{r})$ occurs is Gaussian:

$$P[\rho(\boldsymbol{r})] \sim \exp\left[-\int d^3 r \frac{[\rho(\boldsymbol{r}) - \rho_0]^2}{2\rho_0}\right], \qquad (3)$$

where ρ_0 is the mean density of crosslinks.

It is not possible to directly average the logarithm of the partition function Z and obtain the exact free energy. So an alternative definition of a logarithm (the limit: $\log Z = \partial_m Z^m|_{m\to 0}$) is used, allowing to perform the simpler average of the product Z^m. This way of dealing with quenched disorder is called the "replica trick", first introduced in the context of spin glasses by Edwards and Anderson [35]. The expression for the free energy arising from disorder then reads:

$$\begin{aligned} F_d &= -k_B T \langle \log Z \rangle_{\rho,\mathbf{k}} = -k_B T \frac{\partial}{\partial m} \langle Z^m \rangle \Big|_{m\to 0} \quad (4) \\ &= -k_B T \frac{\partial}{\partial m}\Big|_{m\to 0} \prod_{a=1}^{m} \int D\boldsymbol{n}_a \, \exp\left[-\beta H_{\rm rep}\right] \end{aligned}$$

where we now have m identical"replicas" of the system, labelled by the index a. The aim of this work is to obtain F_d as a function of the order parameter Q and add it to the Landau-De Gennes free energy to see how it influences the phase transition.

A rough sketch of the averaging over disorder is given below. The density average over $P(\rho)$ yields a random field term

$$\sim \exp\left[\sum_{a,b} (\beta\gamma Q)^2 \rho_0 (\boldsymbol{k}_a \cdot \boldsymbol{n}_a)^2 (\boldsymbol{k}_b \cdot \boldsymbol{n}_b)^2\right],$$

where (here and throughout this paper) $\beta = 1/k_B T$. The reader's attention is drawn to the appearance of a second replica index b due to the square of the $\sum_a$. Since the distribution of the orientations of the easy axes $P(\boldsymbol{k})$ is assumed fully isotropic, symmetry arguments show that the average $\langle k_i k_j k_l k_m \rangle_{P(k)}$ is proportional to $(\delta_{ij}\delta_{lm} + \delta_{il}\delta_{jm} + \delta_{im}\delta_{jl})$. The constant of proportionality is equal to $1/(2d + d^2)$, where d is the dimensionality of the unit vector $\boldsymbol{k}$. Therefore

$$\begin{aligned} &\langle e^{k^i k^j k^l k^m \, n^i n^j n^l n^m} \rangle_{P(k)} = \\ &= 1 + \langle k^i k^j k^l k^m \rangle \, n^i n^j n^l n^m + \ldots \\ &\approx e^{\langle k^i k^j k^l k^m \rangle \, n^i n^j n^l n^m}. \end{aligned} \quad (5)$$

Since $(n_a \cdot n_b) \leq 1$ higher terms of the Taylor expansion are smaller than the lowest order term ($(n_a \cdot n_b)^2$) and are subsequently dropped in the last line of Eq. (5). This approximate treatment retains a random field term which is overall fourth order in $\boldsymbol{n}$, as it was before the $\boldsymbol{k}$-averaging, and it is most frequently met, and used, in molecular theories involving rotational diffusion.

The second line of Eq. (4) is obtained after averaging over quenched disorder, sketched above, and provides the definition of the "Replica Hamiltonian", which no longer depends on the quenched distributions of $\{\boldsymbol{k}\}$ and $\rho(r)$, but instead couples different replicas of the system:

$$\begin{aligned} H_{\rm rep}\left[\boldsymbol{n}\left(\boldsymbol{r}\right)\right] \equiv \sum_{a,b=1}^{m} \int d^3\boldsymbol{r} \Big\{ \frac{K}{2} \left(\nabla \boldsymbol{n}_a\right)^2 \delta_{ab} + \\ - \frac{\Gamma}{2} \left[2\left(\boldsymbol{n}_a \cdot \boldsymbol{n}_b\right)^2 + \left(\boldsymbol{n}_a \cdot \boldsymbol{n}_a\right)\left(\boldsymbol{n}_b \cdot \boldsymbol{n}_b\right)\right] \Big\}, \end{aligned} \quad (6)$$

where subscripts a and b are the replica indexes and m is the number of replicas that will be set to zero at the end of the calculation. Parameter Γ, arising from completing the Gaussian square between the Eq. (3) and the random-field term in the Eq. (2), reflects the strength of the disorder and has a quadratic dependance on the order parameter:

$$\Gamma = \frac{\gamma^2 \rho_0}{15\, k_B T} Q^2. \quad (7)$$

It is noted that all replicas are assumed to have equal disorder strength and equal magnitude of the local order parameter, i.e. $\gamma_a = \gamma_b$ and $Q_a = Q_b$ for all a and b. Bearing in mind that the director is a unit vector we see that the term with $(\boldsymbol{n}_a \cdot \boldsymbol{n}_a)(\boldsymbol{n}_b \cdot \boldsymbol{n}_b)$ in the random field part of the Replica Hamiltonian just adds an irrelevant constant to the expression. We drop this term and keep the relevant contribution $-\Gamma\left(\boldsymbol{n}_a \cdot \boldsymbol{n}_b\right)^2$ that describes the coupling between different replicas.

III. DISORDER FREE ENERGY

A. Auxiliary Fields

Care must be taken to ensure that the director $\boldsymbol{n}(\boldsymbol{r})$ remains a unit vector. Although this was assumed to be the case, it has not been implemented explicitly in the Eq. (6). One way to achieve this multiplies the partition function in Eq. (4) with the delta-function constraint

$$\delta\left(\boldsymbol{n}^2 - 1\right) = \frac{1}{2\pi} \int_{-\infty}^{\infty} d\phi \, e^{-i\,\phi\left(\boldsymbol{n}^2 - 1\right)}, \quad (8)$$

where ϕ is an auxiliary field that allows the delta-function to be written in its exponential form. We proceed with a mean-field treatment of the auxiliary fields where a constant value for ϕ is assumed, independent of spacial coordinates. This approximation implies that the constraint $\boldsymbol{n}^2 = 1$ is equally enforced across the whole sample. It is reasonable to expect this, given that the sample is spatially homogeneous. The same reasoning explains why ϕ has no dependance on the replica indexes: since its value is independent of the position of the crosslinks in the sample, it cannot have different values for different replicas. The corresponding quadratic term $\sum_a i\,\phi\left(\boldsymbol{n}_a^2 - 1\right)$ has to be added to the Replica Hamiltonian in Eq. (6).

To obtain the disorder energy one must evaluate the statistical sum over all possible trajectories $\boldsymbol{n}_a$. The standard way to evaluate Hamiltonians with quartic interactions is to introduce an auxiliary field, here a tensor λ_{ab},

which reduces the Hamiltonian to bilinear order in $\boldsymbol{n}_a$. To employ the method all the quantities in $\beta H_{\rm rep}[\boldsymbol{n}(\boldsymbol{r})]$ must be dimensionless. Since the integral over r has the dimensions of volume, we move to a discrete summation over all points in space:

$$\int_a^L dx \int_a^L dy \int_a^L dz \,=\, a^3 \sum_{\text{points r}} .$$

The limits of the r-integration are L, the size of the system, and the short-distance cutoff a – the nematic coherence length, below which the continuum representation is no longer applicable. The (a,b) replica coupling term then becomes

$$\begin{aligned} &\exp\left[\beta\Gamma a^3 \sum_r \left(\boldsymbol{n}_a\cdot\boldsymbol{n}_b\right)^2\right] \qquad (9)\\ &= \int d\lambda_{ab} \exp\left\{\sum_r \left[-\frac{\lambda_{ab}^2}{4\tilde{\Gamma}} + \lambda_{ab}(\boldsymbol{n}_a\cdot\boldsymbol{n}_b)\right]\right\}, \end{aligned}$$

which involves the dimensionless constant $\tilde{\Gamma} = \beta\Gamma a^3$. It is important to clarify the meaning of the λ_{ab}^2 term in Eq. (9): it is the square of the value λ_{ab} rather than an element of the product of two matrices. Furthermore, from now on we shall use a mean-field approximation, where it is assumed that λ_{ab} has no r-dependance. This is an important limitation, but we believe it is reasonable as we are looking for homogeneous ordering in the system. Summation over r of the λ_{ab}^2 term yields $N\,\lambda_{ab}^2/(4\Gamma)$, where $N = V/a^3$ is the number of "discrete spacial points" and $V = L^3$ is the system's volume.

Moving to the corresponding discrete Fourier space, the effective Replica Hamiltonian includes both auxiliary fields:

$$\begin{aligned} \beta H_{\rm eff}\left[\boldsymbol{n}\left(q\right)\right] \,=\, &\sum_{a,b}\Bigg\{ -i\phi\,\delta_{ab} \,+\, N\frac{\lambda_{ab}^2}{4\tilde{\Gamma}} \,+\\ +\, &\sum_q \left[\left(\frac{\tilde{K}q^2}{2} + i\phi\right)\delta_{ab} \,-\, \lambda_{ab}\right]\left(\boldsymbol{n}_a\cdot\boldsymbol{n}_b\right)\Bigg\}, \qquad (10) \end{aligned}$$

with the dimensionless elasticity constant $\tilde{K} = \beta K a^3$. The discrete sum over q is related to the integral via $\sum_q = L^3 \int \frac{d^3q}{(2\pi)^3}$. As mentioned above, the conversion from the integral to the discrete sum is essential so that all the quantities in $H_{\rm eff}$ (such as $\tilde{\Gamma}$, ϕ, λ_{ab} and $\tilde{K}q^2$) remain dimensionless and the logarithm of their sum can be evaluated correctly.

To be able to deduce the disorder energy as a function of the order parameter, we make explicit the dependence of $\tilde{\Gamma}$ and $\tilde{K}$ on the magnitude of the order parameter Q:

$$\begin{aligned} &\tilde{\Gamma} = gQ^2\,, \quad \text{with} \quad g = \frac{(\gamma\beta)^2\rho_0 a^3}{15}\\ &\tilde{K} = \beta\kappa a^3 Q^2\,, \qquad (11) \end{aligned}$$

where $\kappa \sim k_B T/a$ is the Frank elastic constant deep inside the nematic phase. It is worth noting that $\tilde{\Gamma}$ is always significantly smaller than one. The distance between crosslinks, d_c, which can be deduced from the crosslink density $\rho_0 \simeq d_c^{-3}$, is found around $7-10$nm in nematic elastomers [10]. A typical coherence length for nematics is $a \sim 5$nm, hence $(a/d_c)^3 \simeq 0.4$ or less. The coupling of disorder to the nematic director is deduced from the size of the domains in Ref [10] and is found to be $\gamma \simeq 0.4 k_B T$. Therefore this crude estimate gives $g \simeq 4\times 10^{-3}$ for the nematic elastomers studied in the literature.

B. Replica Symmetry Case

To be able to advance in the calculation, a matrix form of the auxiliary field λ_{ab} has to be postulated. A reasonable starting point is to assume that it has the simplest possible form, where its elements have a constant value independent of a and b:

$$\lambda_{ab} \,=\, \lambda\left(\mathbb{1}_{ab} \,-\, \delta_{ab}\right), \qquad (12)$$

where $\mathbb{1}_{ab}$ is the matrix with all its elements equal to one and δ_{ab} is the identity matrix. This scheme is frequently encountered in the literature [36] and is called the "Replica Symmetry" limit. It is important to clarify that we are free to choose any form we like for λ_{ab}, and that we will later come back to this choice and check whether it is appropriate or not, in Section IV. There is an important reason why the diagonal elements of the auxiliary field λ_{ab} are chosen to be zero in Eq. (12). Had $\lambda_{ab} = \lambda\mathbb{1}_{ab}$ been our choice, then the summation over a and b of λ_{ab}^2 would have given $m^2\lambda$. The quadratic dependence on m would have meant that, after differentiating with respect to m and setting $m = 0$, this term would be equal to zero. Clearly this is not acceptable since the introduction of the auxiliary field in Eq. (9) requires a non-zero λ_{ab}^2 quadratic term.

Substituting the replica-symmetric ansatz into the effective Hamiltonian of Eq. (10), we find:

$$\begin{aligned} \beta H_{\rm eff} = \sum_{a,b}\Bigg\{ &-i\phi\,\delta_{ab} + N\frac{\lambda^2}{4\tilde{\Gamma}}\left(\mathbb{1}_{ab} - \delta_{ab}\right) +\\ &+\frac{1}{2}\sum_q G_{ab}^{-1}(\boldsymbol{n}_a\cdot\boldsymbol{n}_b)\Bigg\}, \qquad (13) \end{aligned}$$

where the propagator of the $a-b$ replica coupling is given by:

$$G_{ab}^{-1} \,=\, \left(\tilde{K}q^2 + 2i\phi + 2\lambda\right)\delta_{ab} - 2\lambda\mathbb{1}_{ab}. \qquad (14)$$

A consequence of replica symmetry is that G_{ab}^{-1} only involves matrices δ_{ab} and $\mathbb{1}_{ab}$, and as a result its logarithm is easily obtained:

$$\begin{aligned} \log G_{ab}^{-1} \,&=\, \log\left(\tilde{K}q^2 + 2i\phi + 2\lambda\right)\delta_{ab} +\\ &+\, \frac{1}{m}\log\left(1 - \frac{2\lambda\, m}{\tilde{K}q^2 + 2i\phi + 2\lambda}\right)\mathbb{1}_{ab} \qquad (15) \end{aligned}$$

The path integral over configurations $\boldsymbol{n}_a$ with the statistical weight determined by the effective Hamiltonian (13) is Gaussian and gives $(\mathrm{Det}G^{-1})^{-1/2} = \exp(-\frac{1}{2}\,\mathrm{tr}\log G^{-1})$ for each of the three vector components of $\boldsymbol{n}$. As a result the disorder free energy is given by:

$$\beta F_d \;=\; -\frac{1}{2}\frac{\partial}{\partial m}\int d\lambda \int d\phi\, \exp\Big\{ -\frac{N\lambda^2}{4\tilde{\Gamma}}(m^2-m) + \\ +i\phi m \,+\frac{3}{2}\sum_q \mathrm{tr}\log G^{-1}_{ab}\Big\}\Big|_{m\to 0} \qquad (16)$$

from the three (identical) path integrals for the components of $\boldsymbol{n}$.

C. Disorder Free Energy

The aim of this section is to determine the particular values of the auxiliary fields (λ^*_{ab} and ϕ^*) that make the disorder energy of Eq. (16) a minimum. To treat the problem properly, one would have to evaluate the integrals over λ_{ab} and ϕ, which is analytically challenging. The standard way to bypass this difficulty, is to employ the saddle-point approximation based on the simple observation that the exponentially most significant contribution in Eq. (16) will occur when the exponent is a maximum. Therefore

$$\beta F_d(K,\,\Gamma) \;\approx\; -\frac{1}{2}\frac{\partial}{\partial\, m}\exp\Big\{\min_{\lambda,i\phi}\Big[-\frac{3}{2}\sum_q tr\log G^{-1}_{ab} \\ +im\phi - \frac{N\lambda^2}{4\tilde{\Gamma}}(m^2-m)\Big]\Big\}\Big|_{m\to 0}, \qquad (17)$$

where $\min_{\lambda,i\phi}(..)$ represents the minimum of a function with respect to variations in λ and $i\phi$. After substituting the trace of the logarithm from the Eq. (15), we differentiate with respect to m and then set m equal to zero. The disorder energy then takes the form:

$$\beta F_d \approx \min_{\lambda,i\phi}\Big\{ -i\phi - \frac{N\lambda^2}{4\tilde{\Gamma}} + \qquad (18)$$
$$+\;\frac{3}{2}\sum_q\Big[\log\Big(\tilde{K}q^2+2i\phi+2\lambda\Big) - \frac{2\lambda}{\tilde{K}q^2+2i\phi+2\lambda}\Big]\Big\},$$

and we are left with the task of finding the stationary point $(i\phi^*,\lambda^*)$. From now on we move to the continuum limit of space, where the discrete sum is replaced by $\sum_q \to V\int\frac{4\pi q^2}{(2\pi)^3}dq$ and the coherence length a is taken to zero limit.

1. Optimal $i\phi$ in the absence of disorder

The auxiliary field ϕ ensures that the nematic director is a unit vector. This constraint should of course be enforced whether the disorder is present or not. In fact, there is no physical reason why the inclusion of disorder should significantly alter this constraint. Hence, as a first approximation, we look for the optimum $i\phi^*$ when there is no disorder in the system. Setting both Γ and λ equal zero in the Eq. (18) and differentiating with respect to $i\phi$ we obtain:

$$\frac{\partial F_d}{\partial i\phi} = 0 \quad\Rightarrow \qquad (19)$$
$$1 = \frac{3V}{2\pi^2}\Big[\frac{q_{\max}}{\tilde{K}} - \frac{\sqrt{2i\phi}}{\tilde{K}^{3/2}}\tan^{-1}\left(q_{\max}\sqrt{\frac{\tilde{K}}{2i\phi}}\right)\Big].$$

In the continuous limit of $q_{\max}\to\infty$ and the arctangent is equal to $\pi/2$. This equation can be re-written as

$$\sqrt{2i\phi} = \frac{4\pi\tilde{K}^{3/2}}{3V}\left(-1+\frac{3q_{\max}V}{2\pi^2\tilde{K}}\right). \qquad (20)$$

Clearly the -1 term is negligible compared to $(q_{max}V/\tilde{K})$, and can be therefore neglected. Another factor that supports this omission is that we want to examine what happens close to the phase transition, where $Q\to 0$. In this limit, the elastic constant is known to vanish ($\propto Q^2$) and the term with $\tilde{K}^{-1}$ dominates in the bracket.

Assuming that the inclusion of disorder has only a minor effect on ϕ, the value we will use from now on is:

$$i\phi^* = \frac{2\tilde{K}q^2_{\max}}{\pi^2}, \qquad (21)$$

which tends to infinity in the continuum limit of space. It is interesting to note that very close to the transition the constraint relaxes since $\phi\to 0$. This is not surprising since the meaning of the director itself becomes ill-defined as we approach the transition point.

The full calculation to obtain $\phi^*(\lambda)$ in a system with disorder is possible. However, using a disorder-dependent $\phi^*(\lambda)$ in Eq. (18) makes it analytically impossible to solve $\partial F_d/\partial\lambda = 0$ and determine the optimum λ^*. Even a perturbative approach : $\phi^*(\lambda) = \phi^*_{\lambda=0} +$ "*small correction*" does not help matters. To overcome this difficulty the (ϕ^*,λ^*) saddle point should be found numerically, searching for a global energy minimum in the $Q-\gamma$ space. The important drawback of the latter is that we will then be unable to determine the analytical form of $\lambda^*(Q)$ and therefore the final $F_d(Q)$ correction to the Landau free energy of the phase transition.

2. Optimal λ for weak disorder

We proceed to determine the value of the auxiliary field λ^* that minimizes the energy in the replica symmetric approximation. Differentiating the right-hand side of Eq. (18) and demanding it to be zero we find:

$$\frac{\lambda^* N}{2\tilde{\Gamma}} = \frac{3V}{\pi^2}\int\frac{q^2}{\Big(\tilde{K}q^2+2i\phi^*+2\lambda^*\Big)^2}\,dq\,.$$

Integration over momentum space gives the stationary condition on the auxiliary field:

$$\frac{\lambda^* N}{2\tilde{\Gamma}} = \frac{3V}{\pi^2}\Bigg[- \frac{q_{\max}}{2\tilde{K}(\tilde{K}q_{\max}^2 + 2i\phi^* + 2\lambda^*)} + \frac{1}{(2\tilde{K})^{3/2}\sqrt{i\phi^* + \lambda^*}} \tan^{-1}\left(q_{\max}\sqrt{\frac{K}{2i\phi^* + 2\lambda^*}}\right)\Bigg] \tag{22}$$

In the continuous limit of $q_{\max} = 2\pi/a \to \infty$ the first term vanishes and the arctangent is equal to $\pi/2$. Equation (22) has only one real solution. Unfortunately, its full expression is too long and cumbersome to appear here explicitly; instead we demonstrate its behavior in two limits. Expanded in powers of $\tilde{\Gamma} \ll 1$ (weak disorder) it takes the form

$$\lambda^*(\Gamma) = \frac{3V}{N(2\tilde{K})^{3/2}\pi\sqrt{i\phi^*}}\,\tilde{\Gamma} + \mathcal{O}(\Gamma^2). \tag{23}$$

It is a reassuring property that λ^* vanishes as $\Gamma \to 0$.

Critical to our work is the behavior of λ^* as the order parameter Q tends to zero. Both Γ (from its definition) and K (for small Q) are quadratic functions of Q. Therefore the leading term in the series expansion of small Q is

$$\lambda^*(Q) = \frac{(3V)^{2/3}}{2\pi^{2/3}N^{2/3}}\,\frac{\tilde{\Gamma}^{2/3}}{\tilde{K}} + \mathcal{O}(Q^{4/3}). \tag{24}$$

The scaling $\lambda^* \propto Q^{-2/3}$ is thus obtained, showing that λ^* diverges as the transition is approached, that is, even a weak disorder becomes relevant near the $Q \to 0$ point.

3. Final disorder free energy

To find the final disorder energy the values of fields ϕ^* and λ^* are put back in the Eq. (18). Performing the q-integrations in the continuum limit we obtain:

$$F_d \;=\; -i\phi^* - \frac{N\lambda^*}{4\tilde{\Gamma}} + \frac{V}{12\pi^2}\Bigg[- \frac{6q_{\max}(\lambda^* - 2i\phi^*)}{\tilde{K}} + \frac{3\sqrt{2}\pi\left(\lambda^2 - i\phi^*\lambda^* + 2\phi^{*2}\right)}{\tilde{K}\sqrt{i\phi^* + \lambda^*}}\Bigg] \tag{25}$$

The energy we are interested in arises from disorder and we can safely ignore terms that are still present when $\lambda^* = \Gamma = 0$. At diminishing order parameter, the leading term of Eq. (25) takes the form:

$$F_d = \frac{V(\lambda^*)^{3/2}}{2\sqrt{2}\pi\tilde{K}^{3/2}} \approx \frac{3V^2\tilde{\Gamma}}{8\pi^2\tilde{K}^3 N} \propto Q^{-4}\,, \tag{26}$$

which clearly diverges as $Q \to 0$. This divergence of the disorder free energy implies that the isotropic phase can never be reached and, as we shall see in greater detail in Section V. This in turn leads to the rounding of the nematic-isotropic phase transition. Before all this is discussed, we examine if the replica-symmetric form of λ_{ab} in Eq. (12) was an appropriate choice, which is far from obvious.

IV. STABILITY OF REPLICA SYMMETRY

A. The Hessian

A necessary condition for the replica-symmetric solution to be applicable is that the disorder energy is stable for infinitesimal variations of that solution. The auxiliary field λ^* gives an energy extremum; whether this extremum is a maximum or a minimum is determined by a stability analysis following the work of de Almeida and Thouless in spin glasses [37]. We start by allowing the matrix of the auxiliary field λ_{ab} to deviate from its replica-symmetric form:

$$\lambda_{ab} = \lambda^*\left(\mathbb{1}_{ab} - \delta_{ab}\right) + \epsilon_{ab}\;, \tag{27}$$

with ϵ_{ab} the arbitrary infinitesimal deviation from replica symmetry. The disorder free energy will be expanded to second order in $\boldsymbol{\epsilon}$:

$$F_d(\lambda_{ab}) = F_{RS} + \frac{1}{2}\sum_{abcd} H_{ad,bc}\epsilon_{ab}\epsilon_{cd} \tag{28}$$

where F_{RS} represents the energy of the replica-symmetric case ($\epsilon_{ab} = 0$), given by the Eq. (25). The second-order term in ϵ_{ab} involves the fourth rank tensor of coefficients H_{adbc}, which is called the Hessian. It plays an important role in this analysis, because the replica-symmetric solution is only stable as long as H_{adbc} is positive definite, or equivalently only as long as its eigenvalues are non-negative. Of course there is no term linear in ϵ_{ab} because its coefficient is given by the right hand side of Eq. (22) and is therefore equal to zero.

We proceed to find the Hessian of this model. Expanding the first term of the disorder energy in powers of ϵ_{ab} gives:

$$\frac{N}{4\tilde{\Gamma}}\lambda_{ab}^2 = \frac{N}{4\tilde{\Gamma}}\left(\lambda_{ab}^{rs\,2} + 2\lambda_{ab}^{rs}\epsilon_{ab} + \epsilon_{ab}\epsilon_{ab}\right)\;, \tag{29}$$

where $\lambda_{ab}^{rs} = \lambda^*\left(\mathbb{1}_{ab} - \delta_{ab}\right)$. Hence the contribution to the Hessian from this term is $(N/2\tilde{\Gamma})\,\delta_{ad}\,\delta_{bc}$.

The other contribution comes from the trace of the logarithm. The propagator of Eq. (14) can be written as $G_{ab}^{-1} = \left(\tilde{K}q^2 + 2i\phi\right)\delta_{ab} - 2\lambda_{ab}$, therefore allowing λ_{ab} to vary gives the following form to the propagator

$$G_{ab}^{-1} = G_{ab}^{rs\,-1} - 2\epsilon_{ab}\,, \tag{30}$$

where the replica-symmetric $G_{ab}^{rs\,-1}$ is given in Eq. (14). Therefore,

$$\mathrm{tr}\,\log G_{ab}^{-1} = \mathrm{tr}\,\log\left[G_{ac}^{rs\,-1}\left(\delta_{cb} - 2G_{cd}^{rs}\,\epsilon_{db}\right)\right] \tag{31}$$

where summation over the dummy indexes c, d is implicit and

$$G_{ab}^{rs} = \frac{1}{\tilde{K}q^2 + 2i\phi^* + 2\lambda^*}\,\delta_{ab} + \frac{2\lambda^*}{(\tilde{K}q^2 + 2i\phi^* + 2\lambda^*)^2}\,\mathbb{1}_{ab}$$

is the inverse of Eq. (14). In the case of two commuting matrices: $\log(\boldsymbol{A}\cdot\boldsymbol{B}) = \log(\boldsymbol{A}) + \log(\boldsymbol{B})$. It turns out that the eigenvectors of the Hessian (ϵ_{ab}) indeed commute with matrix G_{ab}. This is largely because the latter is a combination of two very simple matrices $\mathbb{1}_{ab}$ and δ_{ab}. Breaking up the product under the logarithm:

$$\log \boldsymbol{G}^{-1} = \log \boldsymbol{G}^{rs\,-1} + \log(\boldsymbol{\delta} - 2\,\boldsymbol{G}^{rs}\cdot\boldsymbol{\epsilon})$$

and expanding the second term in a Taylor series, we obtain:

$$\begin{aligned}\operatorname{tr}\log G^{-1}_{ab} &= \operatorname{tr}\log G^{rs\,-1}_{ab} - 2\sum_{ab} G^{rs}_{ba}\epsilon_{ab} \\ &\quad -2\sum_{abcd} G^{rs}_{da}\epsilon_{ab}G^{rs}_{bc}\epsilon_{cd}\ . \end{aligned} \tag{32}$$

There are three identical traces to be considered, one for each component of the nematic director. Taking into account the 1/2 factor in front of the Hessian, this contribution is $-6\sum_q G^{rs}_{da}\,G^{rs}_{bc}$ and the overall Hessian takes the form:

$$H_{ad\,bc} = \left(\frac{N}{2\tilde{\Gamma}}\,\delta_{ad}\delta_{bc} - 6\,G^{rs}_{da}G^{rs}_{bc}\right)\,. \tag{33}$$

This Hessian has three distinct values of its many matrix elements, depending on how its many indexes are common to the pairs $\{a,d\}$ and $\{b,c\}$. These values are $H_{aa,bb} = P$, $H_{aa,bc} = H_{ad,bb} = Q$ and $H_{ad,bc} = R$.

B. Hessian Eigenvalues

The eigenvalues of such a 4-rank tensor have been computed by de Almeida and Thouless in their classical work on replica symmetry breaking in spin glasses [37]. For $m \to 0$ only two distinct eigenvalues exist:

$$\Lambda_1 = P - 4Q + 3R \quad \text{and} \quad \Lambda_3 = P - 2Q + R \tag{34}$$

and it is straightforward to obtain them by inserting the appropriate forms of $\boldsymbol{G}^{rs}$ into the expression of the Hessian of Eq. (33). The first eigenvalue

$$\begin{aligned}\Lambda_1 &= \frac{N}{2\tilde{\Gamma}} - 6V\int\frac{4\pi q^2}{(2\pi)^3}\left[\frac{1}{(\tilde{K}q^2+2i\phi+2\lambda)^2}\right. \\ &\qquad \left. -\frac{4\lambda}{(\tilde{K}q^2+2i\phi+2\lambda)^3}\right]dq \\ &= \frac{N}{2\tilde{\Gamma}} - \frac{3(2i\phi+\lambda)V}{8\sqrt{2}\pi\tilde{K}^{3/2}(i\phi+\lambda)^{3/2}}\end{aligned} \tag{35}$$

is degenerate and corresponds to two eigenvectors $\boldsymbol{\epsilon}_1$ and $\boldsymbol{\epsilon}_2$. The first, $\boldsymbol{\epsilon}_1$, is symmetric under interchange of indexes ($\epsilon_{ab} = \alpha$ for all a, b) and determines whether the replica-symmetric fixed point of Eq. (22) is stable or not. In other words, if $\Lambda_1 < 0$ the replica-symmetric solution corresponds to an energy maximum and has no physical relevance.

The remaining two eigenvectors check the general stability of the replica-symmetric scheme. Contrary to $\boldsymbol{\epsilon}_1$, the second eigenvector $\boldsymbol{\epsilon}_2$, corresponding to the degenerate Λ_1, is symmetric under interchange of all but one index ($\epsilon_{ab} = \beta$ for a or $b = c$ and $\epsilon_{ab} = \gamma$ otherwise). This eigenvector is not symmetric and as a result a negative Λ_1 also means that replica symmetry must be broken to determine the correct λ_{ab}. The second eigenvalue is non-degenerate and is given by:

$$\begin{aligned}\Lambda_3 &= \frac{N}{2\tilde{\Gamma}} - 6V\int\frac{4\pi q^2}{(2\pi)^3}\frac{1}{(\tilde{K}q^2+2i\phi+2\lambda)^2}dq = \\ &= \frac{N}{2\tilde{\Gamma}} - \frac{3V}{4\sqrt{2}\pi\tilde{K}^{3/2}(i\phi+\lambda)^{1/2}}\,.\end{aligned} \tag{36}$$

and its corresponding eigenvector, called $\boldsymbol{\epsilon}_3$, also does not have a symmetric form ($\epsilon_{ab} = \delta$ for $a = c$ and $b = d$, $\epsilon_{ab} = \zeta$ for $a = c$ or $a = d$ and $b \neq c, d$, $\epsilon_{ab} = \eta$ otherwise). Similarly to the previous case, if $\Lambda_3 < 0$ then the replica symmetric solution breaks down and different forms of λ_{ab} must be sought.

Accordingly, a sufficient condition for the replica-symmetric solution to be stable is that all the eigenvalues of the Hessian remain positive. Both Λ_1 and Λ_3 show a similar behavior as functions of disorder strength γ, which was defined in the text above Eq. (1), and the order parameter Q. Substituting the optimal ϕ^* and λ^*, we find that when Q does not tend to zero, both eigenvalues remain positive, especially for weak disorder, $\tilde{\Gamma} \ll 1$. As the continuous phase transition is approached and the order parameter diminishes, the three parameters appearing in Eq. (36) become simple functions of Q: $\Gamma \propto Q^2$, $K \propto Q^2$ and $\lambda^* \propto Q^{-2/3}$. Hence, the eigenvalues scale as $Q^{-2} - Q^{-8/9}$ and, therefore, become negative at some point $Q \ll 1$. This means that for $Q \to 0$ the replica-symmetric solution of the auxiliary field Eq. (24) and the resulting expression for the disorder energy, Eq. (26), correspond to an energy maximum and should not be used.

To find the exact point at which replica symmetry becomes unstable we note that it is the second (non-degenerate) eigenvalue, Λ_3 that becomes negative first as $Q \to 0$. Substituting the parameters Γ, K and λ^* we find this crossover value for stability:

$$Q_{\text{stab}} = \frac{3g}{4\sqrt{2}\pi(\beta\kappa a)^{3/2}}\,, \tag{37}$$

where the relation $V/N = a^3$ has been used, with a the short-length cutoff. Bearing in mind that $g \propto a^3$ and that $\kappa \propto 1/a$ we find $Q_{stab} \propto a^3$. To be consistent with previous calculations the continuum limit of space is employed and $a \to 0$. Therefore the threshold value below which replica symmetry breaks tends to zero and the Eq. (24) is always valid in the continuum limit. Another way to see this is by examining the explicit dependance of Λ_3 on the cut-off length-scale a. The first term $(N/\tilde{\Gamma})$ scales as a^{-6} whereas the second term scales as $-a^{-5}$. Therefore when a is taken to zero the first term dominates and the

eigenvalue remains positive. To complete the stability analysis, we note that the other eigenvalue also becomes negative for smaller values of Q when $Q < Q_{stab}/2$, but this is irrelevant since the instability of Λ_3 occurs first.

V. PHASE TRANSITION ANALYSIS

The aim of this paper is to discuss how quenched orientational disorder affects the phase transition of nematic systems. The total free energy density is a combination of the Landau-De Gennes expansion of the order parameter plus the disorder part (F_d/V) obtained in Eq. (25). To get the total energy as an expansion of the order parameter only the leading order contribution of F_d in Eq. (26) is considered:

$$F = \frac{A_0}{2}(T - T^*)Q^2 - \frac{B}{3}Q^3 + \frac{C}{4}Q^4 + \frac{D}{4}Q^{-4}, \quad (38)$$

where

$$D = \frac{3g}{2\pi^2(\kappa\beta a^2)^3}k_B T \quad (39)$$

and A, B, C and T^* are the usual Landau-De Gennes parameters. One may note the explicit dependence of Eq. (39) on the short-length cutoff a and be concerned about the sustainability of the continuum limit $a \to 0$. In fact, because $g \propto a^3$ and $\beta\kappa \simeq 1/a$, the powers of a cancel and the free energy does not depend on this cutoff parameter, which is a reassuring test of consistency of our theory.

The easiest way to illustrate the consequence of the free energy renormalization is to plot the equilibrium values of the order parameter Q. The values chosen for the Landau phenomenological constants are: $A_0 \simeq 5.0 \times 10^3\,\mathrm{Jm^{-3}K^{-1}}$, $B \simeq 3.3 \times 10^5\,\mathrm{Jm^{-3}}$ and $C \simeq 1.0 \times 10^6\mathrm{Jm^{-3}}$. A detailed description on how they are obtained by analyzing experimental data of Ref. [22] is given in the Appendix. We consider these values to be indicative only since different nematic materials will certainly have large variations in these values. Plotting the equilibrium order parameter against reduced temperature, Fig. 2, we can compare $Q(T)$ for the disorder strength increasing from $g = 0$ in (a) up to $g = 10^{-4}$ in (d). As mentioned in Section III a typical polydomain elastomer should have $g \simeq 4 \times 10^{-3}$ and therefore the model predicts a supercritical behavior in agreement with many experiments. Note that in contrast to this result, the quenched orientational disorder was shown not to alter the continuous nematic phase transition in thin films, whose director is confined in the XY-plane [38].

The inclusion of disorder has a profound effect on the phase behavior of 3D systems whose pure versions undergo a first order phase transition. The discontinuous jump of the order parameter at the nematic transition becomes smaller as the strength of the disorder g increases and eventually disappears altogether above a critical value making the phase transition continuous. The

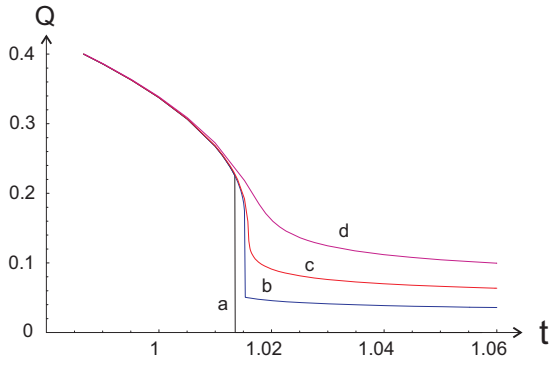

FIG. 2: The equilibrium order parameter Q as a function of reduced temperature $t = T/T^*$ for a range of different disorder strength g. (a) is the first order transition for a system with no disorder (b) is a subcritical system (c) is a critical system (d) is a supercritical system. As the disorder strength increases the discontinuous jump decreases and eventually disappears.

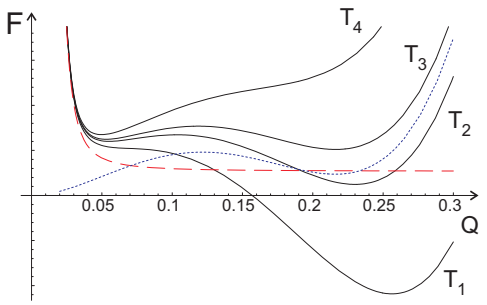

FIG. 3: Free energy against order parameter plots for a subcritical system for a range of temperatures, $T_1 < T_2 < T_3 < T_4$. The doted and dashed lines show respectively the Landau and disorder energies for $T = T_3$. They illustrate that the high-Q minimum is a product of the Landau energy exclusively, whereas the low-Q minimum arises from competition of the AQ^2 Landau term and the disorder energy.

change in behavior is explained by the simple fact that the energy terms arising from disorder scale as negative powers of Q. As a direct result, the energy of the system increases as the transition approaches and the zero order parameter phase is never reached. To see exactly how this happens consider plots of $F(Q)$ of a subcritical and a supercritical system.

For a subcritical system, where disorder is weak, the jump in $Q(T)$ is still present, albeit smaller than in the original transition of the pure system. Because parameter g is small, the disorder part of the energy becomes significant only for small Q, where it diverges. The appearance of the jump has the same origins as in the classical Landau-De Gennes theory. Fig. 3 shows plots of the energy density against order parameter for four different temperatures around T_{NI}. At the lowest temperature (T_1) the single minimum determines the equilibrium

value of Q. As the temperature increases the high-Q minimum moves to a slightly smaller value of Q and - more importantly- another "low-Q" minimum appears as a result of disorder. At T_2 the high-Q is still the global minimum, but at the critical temperature (T_3) the two minima have the same energy value. This means that two distinct phases, one with $Q \simeq 0.23$ and the other $Q \simeq 0.05$, coexist. Once this temperature is passed (T_4) the low-Q minimum determines the system's order parameter. The crucial difference between these plots and the classical Landau-De Gennes theory is that the low-Q minimum in the latter is always placed at $Q = 0$. Since the disorder energy diverges at zero Q, this minimum is pushed at positive values of Q in systems with quenched disorder.

The dotted and dashed lines show the Landau and the disorder energy for the same temperature T_3, respectively. Around the high-Q minimum the dotted line has the same shape as the actual energy; apart from a constant shift to lower energy they are exactly equal. Therefore this minimum is a result of the competition of the $-B\,Q^3$ and $C\,Q^4$ energy terms of the Landau expansion, which dominate at large Q. The position of the low-Q minimum is influenced by disorder. This minimum is a balance of the divergent F_d term and $A\,Q^2$. For temperatures well above T_{NI} the minimum is located at very small order parameter and the only relevant terms of Eq. (38) are DQ^{-4} and $A\,Q^2$.

In a supercritical system disorder is stronger (large g) and therefore its effect on the energy is more prominent. As a result the effect of F_d is relevant for all the values of Q, not just in the small order parameter region as in the previous case. Fig. 4 shows the relevant energy plots. Crucially there is only one minimum at any given temperature. Its position shifts to smaller order parameter as temperature increases, but the phase transition is continuous. In comparison with Fig. 3, we can say that the low-Q minimum has "broadened" and "absorbed" the high-Q minimum.

Another difference with the small g case is that, because F_d has larger magnitude, the low order $A\,Q^2$ term of the Landau expansion does not influence the position of the minimum. The dotted lines in Fig. 4 are drawn for the same temperature as in the previous case of Fig. 3, but now this temperature is labeled as T_1. In this supercritical system the energy minimum occurs at approximately the same value of order parameter as the high-Q minimum of the Landau DeGennes expansion (thin-doted line). In a pure system this would be a metastable state because there would exist a global minimum at $Q = 0$.

The natural question to ask next is what is the critical point at which the jump in $Q(T)$ disappears completely. At this point the free energy must have the merging of all its minima and maxima. Solving for the first, second and third derivatives being zero provides three equations for the unknown critical parameters g_c, T_c and Q_c and

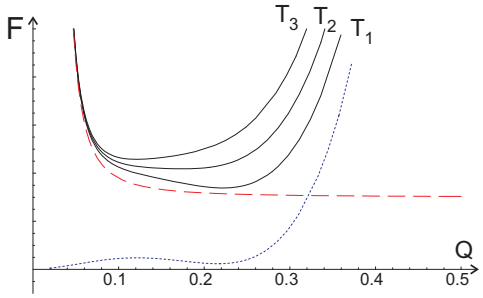

FIG. 4: Energy against order parameter plots of a supercritical system for a range of temperatures, $T_1 < T_2 < T_3$, all larger than T_{NI}. The dotted and dashed lines show the Landau and disorder energies for T_1, respectively. Since the disorder energy diverges the $A\,Q^2$ Landau term is no longer significant.

the critical point is then given by:

$$(g_c, Q_c) = \left(\frac{2\pi^2 7^{11} B^{12} (\kappa\beta a)^3}{916^{12} C^{11}} \,,\, \frac{7B}{16C} \right) . \qquad (40)$$

It is worth comparing this with the classical case of an applied field, which adds a $-f\,Q$ term in the Landau expansion, where the critical Q is slightly smaller and equal to $B/3C$.

In the analysis of the replica symmetry stability in Section IV we found that the above description of nematic systems breaks down for small order parameter when $Q < Q_{\rm stab}$, see Eq. (37). The threshold value of $Q_{\rm stab}$ is proportional to the cube of the cut-off length a. In order to be consistent with the line adopted in previous calculations, the continuum limit of space was employed and a was taken to zero. Hence $Q_{\rm stab}$ was also taken to be zero. However, in reality the length scale a is in fact the nematic coherence length, because below this size we cannot write Frank elasticity and there is no meaning to order parameter Q, or director $\boldsymbol{n}$. Keeping a non-zero, and assigning it the value of 5nm which is usually associated with liquid crystals, makes $Q_{\rm stab}$ also finite. Nevertheless substituting the value of $g \simeq 3\times10^{-3}$ and $\kappa \simeq k_B T/a$ gives $Q_{\rm stab} \simeq 2 \times 10^{-4}$. This is an extremely small value for the order parameter and, as we see from Fig 2, it would only be acquired at temperatures well above the experimental range. Hence, even if $a \neq 0$, the window of replica symmetry stability is wide enough to describe realistic nematic systems.

VI. SUMMARY

This paper examines how the inclusion of randomly quenched orientational disorder leads to the rounding of the nematic-isotropic phase transition in three dimensions. The coupling between impurities and the local order parameter pins some mesogenic molecules and does not allow the sample to have a uniform director field $\boldsymbol{n}(r)$.

After quenched disorder has been averaged over using the replica method, a replica-symmetric auxiliary field is used to obtain the free energy arising from disorder. The disorder energy adds a $\propto Q^{-4}$ term to the Landau-De Gennes expansion which diverges for diminishing order parameter Q. As a result the isotropic phase is never reached and, for sufficiently strong disorder, the phase transition becomes continuous. This is in accordance with many experiments on nematic elastomers that also show a smooth transition rather than a discontinuous as predicted by the classical Landau-De Gennes theory. An earlier study on XY nematics, whose director is confined to a plane, showed that the quenched disorder does not affect their continuous phase behavior [38].

A stability analysis shows that the replica-symmetric solution we have employed does fail at small values of the order parameter, at $Q < Q_{stab}$. However, for realistic values of physical parameters we estimate the order of $Q_{stab} \approx 10^{-4}$ in nematic elastomers. A supercritical system acquires such low values of Q at temperatures well above the elastomers melting point and therefore the window of replica symmetry stability adequately describes the 3D nematic system.

Acknowledgments

We would like to thank Isaac Pérez Castillo, David Sherrington, Paolo Biscari and Raphael Blumenfeld for their feedback. This work has been supported by the Leventis foundation, the Cambridge European Trust and the EPSRC TCM/C3 Portfolio grants.

APPENDIX

In order to determine the three phenomenological parameters A_0, B and C of the Landau-De Gennes theory, defined in Eq. (38), we need three independent measurements. These are provided by a NMR experiment measuring the order parameter as a function of temperature of a polymer melt and its corresponding crosslinked network (a polydomain nematic elastomer) [22]. As expected from the Landau-De Gennes theory, the melt shows a first order transition with the discontinuous jump in order parameter being approximately $\Delta Q \simeq 0.22$, which is smaller than 0.4, the value usually associated with ordinary liquid crystals [39]. The theoretical prediction gives this jump to be equal to $\Delta Q = 2B/3C$ [14] and substituting the experimental measurement we find $B \simeq 0.33C$. The second measurement is the width of the temperature hysteresis which is $\Delta T \simeq 5K$ in the polymer melt. Theory predicts $\Delta T = 2B^2/9A_0C$. Combining this with $B \simeq C/3$ we find $B = 67\,A_0\ 1K$ and $C = 200\,A_0\ 1K$. To get a value of A_0 a third measurement is required.

A striking difference between the two $Q(T)$ plots, for a nematic polymer melt and its crosslinked elastomer version, is that crosslinking has reduced the overall order at temperatures below T_{NI}. For elastomers crosslinked in the isotropic phase, the energy addition arising from nematic rubber elasticity adds a fourth order term in the Landau expansion [40]:

$$\frac{3}{4}\,\mu\,\alpha^4\,Q^4$$

where μ is the rubber modulus and α accounts for the microscopic details of an elastomer. For a freely joined polymer $\alpha = 3$ [11], but a side-chained polymers have α ranging between -0.5 and 0 [41]. Let us take an intermediate case where $\alpha = 1$. When this term is added to the Landau-De Gennes expansion, the fourth-order coefficient (which is $C/4$ for the polymer melt) now becomes larger $\frac{C}{4}(1 + 3\mu\alpha^4/C)$. Hence the transition temperature, given by $T_{NI} = T^* + 2B^2/3A_0C^2$, decreases since the renormalized C increases. The shift in this transition temperature between the melt and the corresponding elastomer is:

$$\Delta T_{NI} \;=\; -\frac{2\,B^2\,\mu\,\alpha^3}{3\,A_0\,C^2}\ . \qquad \text{(A.1)}$$

and it provides the third relation that allows to determine A_0. An estimate of ΔT_{NI} is possible in Ref [22]: T_{NI} is easily identified in the polymer melt, but it is not clear what it means in the disordered nematic elastomer with a continuous transition. It can be loosely defined as the temperature where $Q = \Delta Q = 0.22$. This then makes $\Delta T_{NI} \simeq 15^o\,C$. Substituting this back to Eq. (A.1) with $\alpha = 1$, we obtain $A_0 \simeq \frac{\mu}{200\ K}$. A typical nematic elastomer has elastic modulus of the order of 10^6 Pa. Putting everything together, the phenomenological constants of a nematic elastomer are:

$$A_0 \simeq 5.0 \times 10^3\,\mathrm{Jm^{-3}}K^{-1},\quad B \simeq 3.3 \times 10^5\,\mathrm{Jm^{-3}}$$
$$\text{and}\quad C \simeq 1.0 \times 10^6\mathrm{Jm^{-3}}.$$

These values are crude estimations, only given here to illustrate the effect of disorder in our model. However, it is comforting that, although obtained from a different set of experimental measurements, these values are quite close to the ones reported in literature [11].

[1] Y. Imry and M. Wortis, Phys. Rev. B **19**, 3580 (1979).

[2] M. Aizenman and J. Wehr, Phys. Rev. Lett. **62**, 2503 (1989).

[3] J. Cardy, J. Phys. A-Math. Gen. **29**, 1897 (1996).

[4] J. Cardy, Physica A **263**, 215 (1999).
[5] E. M. Chudnovsky, W. M. Saslow, and R. A. Serota, Phys. Rev. B **33**, 251 (1986).
[6] D. E. Feldman, Phys. Rev. B **61**, 382 (2000).
[7] T. Bellini, R. Clark, and S. D.W., Phys. Rev. Lett. **74**, 2740 (1995).
[8] T. Bellini, M. Buscaglia, C. Chiccoli, F. Mantegazza, P. Pasini, and C. Zannoni, Phys. Rev. Lett. **85**, 1008 (2000).
[9] Y. Imry and S. Ma, Phys. Rev. Lett. **35**, 1399 (1975).
[10] S. V. Fridrikh and E. M. Terentjev, Phys. Rev. E **60**, 1847 (1999).
[11] M. Warner and E. M. Terentjev, *Liquid Crystal Elastomers* (Oxford Science Publications, Oxford (U.K.), 2003).
[12] S. M. Clarke, E. M. Terentjev, I. Kundler, and H. Finkelmann, Macromolecules **31**, 4862 (1998).
[13] S. M. Elias, F.and Clarke, R. Pech, and E. M. . Terentjev, Europhys. Lett. **47**, 442 (1999).
[14] P. G. de Gennes and J. Prost, *The Physics of Liquid Crystals* (Oxford Science Publications, Oxford (U.K.), 1995).
[15] I. Chuang, N. Turok, and B. Yurke, Phys. Rev. Lett. **66**, 2472 (1991).
[16] A. I. Larkin, Sov. Phys-jetp. Engl. Trans. **31**, 784 (1970).
[17] E. M. Chudnovsky and R. A. Serota, Phys. Rev. B **26**, 2697 (1982).
[18] D. J. Cleaver, S. Kralj, T. J. Sluckin, and M. P. Allen, Appears in: Liquid crystals in Complex Geometries formed by polymer and porous networks (1997).
[19] S. V. Fridrikh and E. M. Terentjev, Phys. Rev. Lett. **79**, 4661 (1997).
[20] P. Olmsted and E. Terentjev, Phys. Rev. E **53**, 2444 (1996).
[21] H. Stark and T. Lubensky, Phys. Rev. E **55**, 514 (1997).
[22] S. Disch, C. Schmidt, and H. Finkelmann, Macromol. Rapid Commun. **15**, 303 (1994).
[23] A. Lebar, Z. Kutnjak, S. Zumer, H. Finkelmann, A. Sanchez-Ferrer, and B. Zalar, Phys. Rev. Lett. **94**, art. no. (2005).
[24] W. Kaufhold, H. Finkelmann, and H. R. Brand, Makromol. Chem-macro. Chem. Phys. **192**, 2555 (1991).
[25] J. Kupfer and H. Finkelmann, Macromol. Chem. Rapid. Commun. **12**, 717 (1991).
[26] H. Finkelmann, A. Greve, and M. Warner, Eur. Phys. J. E **5**, 281 (2001).
[27] S. M. Clarke, A. Hotta, A. R. Tajbakhsh, and E. M. Terentjev, Phys. Rev. E **6406**, art. no. (2001).
[28] J. V. Selinger, H. G. Jeon, and B. R. Ratna, Phys. Rev. Lett. **89**, 225701 (2002).
[29] N. Uchida, Phys. Rev. E **62**, 5119 (2000).
[30] J. V. Selinger and B. R. Ratna, Phys. Rev. E **70**, 041707 (2004).
[31] P. Pasini, G. Skacej, and C. Zannoni, Chem. Phys. Lett. **413**, 463 (2005).
[32] G. C. Verwey and M. Warner, Macromolecules **30**, 4196 (1997).
[33] Y. O. Popov and A. N. Semenov, Eur. Phys. J. B **6**, 245 (1998).
[34] X. Xing and L. Radzihovsky, Phys. Rev. Lett. **90**, 168301 (2003).
[35] S. F. Edwards and P. W. Anderson, J. Phys-f-metal. Phys. **5**, 965 (1975).
[36] V. Dotsenko, *Introduction to the Replica Theory of Disordered Statistical Systems* (Cambridge University Press, Cambridge (U.K.), 2001).
[37] J. R. L. de Almeida and D. J. Thouless, J. Phys. A-Math. Gen. **11**, 983 (1978).
[38] L. Petridis and E. M. Terentjev, J. Phys. A: Math. Gen. **39**, 9693 (2006).
[39] J. Shen, N. A. Clark, P. S. Pershan, and E. B. Priestley, Phys. Rev. Lett. **31**, 1552 (1973).
[40] M. Warner, K. P. Gelling, and T. A. Vilgis, J. Chem. Phys. **88**, 4008 (1988).
[41] G. R. Mitchell, M. Coulter, F. J. Davis, and W. Guo, Journal de Physique II **5**, 1121 (1992).